

## Exploring Turbulent Effects on Spray Evaporation Modeling

Noor M. Jasim\*

Received on: 29/12/2010

Accepted on: 6/10/2011

### Abstract

In this work, numerical investigations are conducted for diesel spray under evaporating conditions. The Eulerian-Eulerian framework of evaporating turbulent spray is presented in terms of the methodology of spray moments of drop size distribution. Turbulence effects on mass and heat transfer in evaporation test case are presented. The simulated results showed that the turbulence intensity decreases with the development of spray under hydrodynamic changes. The simulation shows good agreement with the experimental results illustrated by comparison of spray tip penetration elevations.

**Keywords :** Spray modeling, Heat and mass transfer, Turbulent flow

### بحث تأثيرات الاضطراب على نمذجة تبخير الرذاذ

#### الخلاصة

في هذا العمل، تحقيقات عددية أجريت على رذاذ الديزل تحت ظروف التبخير. إن صيغة Eulerian- Eulerian لتبخير الرذاذ المضطرب قدمت بصيغة منهجية لزخم الرذاذ لتوزيع حجم القطرة. هذا البحث أخذ بالاعتبار تأثيرات الاضطراب على انتقال الحرارة والكتلة في حالة اختبار التبخير. أن نتائج المحاكاة أوضحت بأن شدة الاضطراب تتناقص مع تطور الرذاذ تحت التغييرات الهيدروديناميكية. أن المحاكاة أظهرت مقارنة جيدة مع النتائج التجريبية المبينة بالمقارنة لمستويات نفاذ حافة الرذاذ.

### Nomenclature

Symbols	Unit	Description
$B_m$	--	Spalding mass transfer number
$c_p$	( kj/kg.K )	Specific heat
$g$	--	The subscript for the gas
$k$	( kj/m <sup>2</sup> .K )	The thermal conductivity
$L(T)$	( kJ/kg )	the latent heat of evaporation
$\dot{m}_d$	( kg )	The mass lost from a droplet
$n(r)$	--	The droplet number

\*Engineering College, University of Kufa/Kufa

3097

$N(r)$	--	The droplet number probability.
$Q_i$	--	moment of the distribution function
$Q_{c,a}^*$	( kJ )	convective heat transfer
$q_E$	( kJ )	the source term for evaporation
$\dot{q}_m$	( kg )	desired mass source term
$r$	( m )	droplet radius
$s$	--	drop surface conditions
$T$	( K )	Temperature
$V$	( m <sup>3</sup> )	Volume
$x$	--	axial cross section
$\Theta$	--	the gas volume fraction
$\Omega$	( m <sup>3</sup> )	volume

## 1. Introduction

Numerical simulations of spray evaporation under relatively high pressure conditions in industrial engineering applications relevant to gas turbine combustor or diesel engines stills a hard task. This is because constituting a complex phenomena involving the coupling between liquid and gas phases. The principle in all practical devices, the spray as bulk of liquid is delivered at a certain velocity. Whether the gas phase is injected around or with liquid stream or stagnant shear stresses induced by droplets motion lead to the primary atomization and destabilization ended with secondary breakup. Further ligaments and droplets are breaking down when Weber number exceeds the critical value which is based on the local droplet size and relative velocity between drops and the gas phase.

In order to describe the complicated spray, three main mathematical

frameworks have been adopted: the first one is the Eulerian-Eulerian approach; the second one is the Eulerian-Lagrangian approach (also known as Discrete Droplet Modelling, DDM); the last one is the Droplet Distribution Function approach (DDF) which offers a probabilistic formulation to the spray simulation problem.

The Eulerian-Eulerian (or Continuum-Continuum) approach considers both phases to be a continuous fluid interacting and interpenetrating on the same computational grid, Mostafa and Elghobashi [2]. In this approach, the behaviour of dispersed and gas phase is characterized by using the partial differential Navier-Stokes equations which describe the flow of fluid. This leads to a great number of transport equations to be solved if the polydisperse behaviour of the spray is to be interpreted by the introduction of numerous droplet size classes (i.e. a transport equation has to be written for

each size class). Based on the continuum assumption of the disperse phase, Batchelor [3] reported that liquid phase can apply to this approach. Lumley [4] argues that each computational cell must contain a large number of droplets in order to assign statistically averaged properties, such as density or velocity, to the droplets.

The simplest model for characterising the evaporation of a droplet is based on the rate of vaporising governed by the diffusion process. The fact that droplets exchange heat and mass simultaneously with the gaseous phase highlights the complex nature of these interdependent processes. Mostafa and Mongia [5] applied both Eulerian and Lagrangian approaches separately to simulate a turbulent evaporating model for spray.

Hallmann et al. [6] handled used an Eulerian versus Lagrangian approach for modelling turbulent evaporating sprays, through the solution of two transport equations for droplet temperature and diameter.

A uniform temperature model was used by Ma et al. [7], Kim et al. [8] and Caraeni et al. [9] which assumes an infinite thermal conductivity. Their applications of the model were based on a single fuel droplet evaporating assuming that spray droplets are dispersed. Other assumptions include droplets are spherical in shape, constant density with homogeneous temperature.

The work of Ma et al. [7] used (k-ε) model with a modification through an assumption that turbulence kinetic energy is produced only by gas phase and the spray droplets share it. Thus, the dissipation energy equation remains invariant and the k-equation has been changed to cover their assumption.

In this work, studying of numerical simulations of spray evaporation under relatively high pressure conditions in industrial engineering applications relevant to gas turbine combustor. Also, turbulence effects on mass and heat transfer in evaporation test case are studied.

## 2. The Two-phase model

### 2.1. Spray moments theory

Beck and Watkins [1] presented their approach based on the droplet number size distribution,  $n(r)$ , which defined as a multiple of the droplet number probability distribution by droplet radius as below

$$n(r) = \int_{r_m^{ix}}^{r_m^{ax}} N(r) dr \quad (1)$$

Where  $N(r)$  is the droplet number probability distribution. The integral over all droplets provides the total number of droplets per unit total volume (not unit liquid volume). This can be defined as below:

$$Q_0 = \int_0^{\infty} n(r) dr \quad (2)$$

This is the first moment of the distribution function. In this approach, the three remaining distribution function moments are defined as below:

$$Q_i = \int_0^{\infty} r^i n(r) dr \quad (3)$$

At a particular point in space and time,  $Q_0$  is the total number of drops present,  $Q_1$  is the total sum of radii of the drops,  $4\pi Q_2$  is the total surface area of the drops and  $4\pi Q_3/3$  is the total volume of the drops, all quantities within a unit volume of the gas/liquid mixture. The fourth moment is related to the liquid

volume fraction via the following relation

$$\frac{V_{liquid}}{V_{liquid} + V_{gas}} = \frac{4p}{3} Q_3 = 1 - \Theta \quad (4)$$

where  $\Theta$  is the gas volume fraction.

### 2.2. Construction transport equations

This section describes the transport equations for the moments, momentum and energy. The fourth moment-average velocity is treated separately as it is the mass- average velocity, used in the liquid phase momentum and continuity equations. To derive this relationship, first consider an equation for a group of liquid droplets with similar properties as would be solved in a multi-size Eulerian treatment; thus for a droplet group  $k$  occupying volume fraction. This equation can be re-expressed in terms of the number and radius of the droplets in this group. Assuming, the number of droplets in each size group is small and sum over all groups. However according to the definition of the spray moments, it can be rewritten in general form as,

$$\frac{\partial}{\partial t} \int_{\Omega} X Q_i d\Omega + \int_S [V_{d,i} \cdot \vec{n}] X Q_i dS = \int_{\Omega} \Gamma_X grad (X Q_i) d\Omega + \int_{\Omega} q X Q_i d\Omega \quad (5)$$

Thus, when  $X = 1$  is solving for moments,  $X = U_i$  is solving for momentum and  $X = E_i$  is solving for energy. The last term in the above equation represents the source term of the mass transferred by evaporation from this group of droplets to the gas phase per unit volume in case of the fourth moment and represents the heat transferred between the two-phase in case of energy transport equation.

Therefore the next section these two terms are presenting with details. In the two phase flow problem, the interactions between liquid and gas phase are involved. To accomplish this, the parameter which relates between liquid and gas phase is introduced, namely gas volume fraction given by equation(4). Similarly all of the gas phase transport equation can be written in general form as

$$\frac{\partial}{\partial t} \int_{\Omega} Y \Theta d\Omega + \int_S [V_g \cdot \vec{n}] Y \Theta dS = \int_{\Omega} \Gamma_Y grad (Y \Theta) d\Omega + \int_{\Omega} q Y \Theta d\Omega \quad (6)$$

where  $Y$  can be any conserved variable as stated for  $X$

### 2.3. Turbulence model

The  $k-\epsilon$  turbulence model of Launder and Spalding [10] is used here. This model solves transport equations for the turbulence kinetic energy and its dissipation rate. The transport equation for the turbulent kinetic energy is expressed as: The equations are:

$$\frac{\partial}{\partial t} \int_{\Omega} r(1-\Theta) k d\Omega - k q_{Q_i} + \int_S r(1-\Theta) k \vec{u} \cdot \vec{n} dS = \int_S \Gamma_f (1-\Theta) grad k \cdot \vec{n} dS + (1-\Theta) P_k - (1-\Theta) r_g e \quad (7)$$

and;

$$\begin{aligned} & \frac{\partial}{\partial t} \int_{\Omega} r(1-\Theta) e \, d\Omega - e \, q_{Q_i} + \\ & \int_S r(1-\Theta) e \, \vec{u} \cdot \vec{n} \, dS = \\ & \int_S \Gamma_f (1-\Theta) \, \text{grad } e \cdot \vec{n} \, dS \\ & + (1-\Theta) C_{e,1} P_k \frac{e}{k} - (1-\Theta) C_{e,2} r_g \frac{e^2}{k} \\ & + (1-\Theta) C_{e,3} r_g e \, \text{grad } u \end{aligned} \quad (8)$$

The turbulence kinetic energy production rate is given by:

$$P_k = r_g C_m \frac{k^2}{e} (\text{grad } (\bar{u}))^2 \quad (9)$$

The constants take the values [10] :  $C_{\epsilon,1} = 1.44$ ,  $C_{\epsilon,2} = 1.92$ ,  $C_{\epsilon,3} = -0.373$  and  $C_{\mu} = 0.09$ . The term involving  $C_{\epsilon,3} = -0.373$  is an additional term represents the effect of the liquid phase on the gas phase turbulence.

#### 2.4. Heat and mass transfer models

The evaporation of droplets is caused by heat and mass transfer between the droplets and the surrounding gas. Various models are found to describe the deviation of phase transition on the droplet surface i.e., the transport processes inside the droplet and the two phase interfacial interaction. The mass lost from a single droplet then can be written as:

$$\dot{m}_d = 4p \left( \frac{k_g}{c_{p,g}} \right) r_s \ln(1 + B_m) \quad (10)$$

Where  $k$ ,  $c_p$  and  $B_m$  are the thermal conductivity, specific heat and Spalding mass transfer number respectively. The  $g$  subscripted value denotes conditions in the surrounding gas. To obtain the desired mass source term, integrating the mass lost over all droplets gives :

$$q_m = \int_0^{\infty} 4p \left( \frac{k_g}{c_{p,g}} \right) \ln(1 + B_m) * r_s n(r_s) dr_s \quad (11)$$

where  $s$  denotes drop surface conditions. The heat penetrates into the liquid phase during the heat up period when the liquid is not at the saturation temperature. The particular model adopted here is that due to Beck and Watkins [11] in which the convective heat transfer for a single drop is given by:

$$\dot{Q}_{c,d} = \dot{m}_d \left[ \frac{c_{p,g} (T_g - T_s)}{B_m} - L(T_s) \right] \quad (12)$$

where  $L(T)$  is the latent heat of evaporation. Then the source term for evaporation is obtained by integrating over all droplets given by

$$q_E = - \int_0^{\infty} 4p k_g \ln(1 + B_m) * TR * n(r_s) dr_s \quad (13)$$

Where;

$$TR = \left[ \frac{(T_g - T_s)}{B_m} - \frac{L(T_s)}{c_{p,g}} \right] * r_s \quad (14)$$

Notably, the occurrence of the minus sign of the source term implies that the energy is gained by the gas phase, and lost by the liquid phase. In case of mass transfer, it can be assumed that the liquid gains from the gas exactly the energy it requires to evaporate the appropriate amount of mass. Hence the source term  $q_E$  become zero in this case as the net transfer of energy to the liquid is exactly zero.

#### 3. Test Case

According to the experiments of Levy et al. [12] the non-reactive diesel

spray is tested in a constant volume combustion chamber. Droplet sizes and velocities are measured using Particle Doppler Analyzer instrumentation. The injection pressure starts at 17 MPa and varies with needle position in nozzle. The trapped pressure is 2 MPa and the nozzle diameter is 0.2mm. This tests is carried out for different initial gas phase temperatures but one case here is adopted where the initial gas temperature is 443 K within the range of the liquid injection temperature of 298 K.

#### 4. Solution Scheme

A Fortran computer code based on a finite volume method, which uses to solve the integral form of the transport equations as its starting point. The solution proceeds at each time are presented in Fig.1 .The finite volume method is employed to carry out the solution of the transport equations system in an Eulerian-Eulerian framework.

The equations are all solved on the same two-dimensional axisymmetric orthogonal computational grid as shown in Fig.2. The collocated grid approach is used, which involves defining a central control volume for the gas pressure and other scalar variables, including the moments and displaced volumes for the gas and liquid velocities.

The temporal differencing is performed using the Three Time Level method which is a second order implicit scheme and has no time step constraint. This is marginally more complex than the Euler scheme and results in a fully implicit scheme that allows larger time steps to be taken before the scheme becomes unstable. This is generally a good idea in the modelling of spray flows, as a fine grid is required around the nozzle region in order to resolve the large dependency

on inlet conditions. An explicit scheme, for stability, requires prohibitively small time steps.

This is especially the case when considering the large injection velocities of high-pressure diesel sprays and when the very small dimensions of the injector, of  $O(10^{-4})m$ , are discretised into a number of injection cells, as done here. Spatial discretisation of the velocity equations for both phases and the turbulence model equations is done using the upwind scheme. To enhance the stability of the computational calculations the central differencing scheme is used for moments, vapour mass fraction and energy equations.

#### 5. Results and discussion

Spray tip penetrations obtained from the experiment were measured by Phase Doppler Anemometry (PDA). It is simple to define the spray penetration as the furthest distance that liquid droplets reach through a certain time. In this work, calculations used the liquid volume fraction to determine the spray penetration. The comparison results between predicted and experimental data of spray penetration are presented in Fig.3. The agreement is fairly good, with slightly under-predicted along the spray calculations. From penetration results the good agreement can be seen between the experimental and predicted results. This validates the momentum transfer model as this is the key parameter determining the predicted spray penetration. Clearly the predicted values of the moments seem to be acceptable for the modeling to be able to produce penetration results of this accuracy.

The computed profiles of gas axial and radial gas velocities are shown in Fig.4a and b, in which three different axial cross sections are selected to

present these calculations downstream. It was found that the maximum axial gas velocity at  $x=10$  mm due to the high injection velocity. In contrast the lowest values of radial gas velocity were found at  $x=10$  mm because the spray cone angle is relatively small as set in the experiment about  $11^\circ$ . At  $x=20$  mm and 30 mm the effects of droplet dispersion, drag and breakup will be appeared clearly where the reduction in both axial and radial components are taken place.

Fig.4b shows that the radial velocity is negative near the injector at  $x=10$  mm and then is positive at  $x=20$  mm and 30 mm because the development of the recirculation region downstream of the nozzle inside the core of the spray.

The effect of high injection velocity for the spray (liquid) which is reached to 134 m/sec on the carrier phase (gas) is modeled using the well known two-equation model ( $k-\epsilon$ ). Fig.5 a and b show at three different axial cross sections at time 2 ms the radial profiles for the two poles of the model. Again the maximum turbulent kinetic energy is recorded at  $x=10$  mm that is matching the axial gas velocity profile as shown in Fig.4a. As expecting due the highest values of turbulent kinetic energy at  $x=5$  mm the highest values of turbulent dissipation energy because it totally depending the production part as shown in Fig5b. As noted above the turbulence is reduced due to the hydrodynamic and thermodynamic effects as it observed at  $x=10$  mm and 15 mm respectively.

The differences between gas velocity components (axial and radial) and the turbulence model used in the present calculations because the gas velocity values are extracted from the gas momentum equation and the turbulent kinetic energy and turbulent dissipation energy rate values are taken

from equations (7) and (8). Physically the turbulent gas velocity is considered as a combination of two components the gas velocity and its fluctuation.

## 6. Conclusions

In the present work, it can be concluded that the two-equation model performs well with the discrepancy of effect of dispersed phase on the continuous phase. Unfortunately there is a lack in experimental data that can benefit from measuring some parameters related to the mass transfer like vapour mass fraction to validate the model performance.

## References

- [1] J. C. Beck and A. P. Watkins. On the development of a spray model based on drop-size moments. Proc. R. Soc. Lond., A(459)(2003),1365-1394.
- [2] A. A. Mostafa and S. E. Elghobashi. A Two-Equation Turbulence Model for Jet Flows Laden with Vaporizing Droplets. International Journal of Multiphase Flow,11(1985),515-533.
- [3] G. K. Batchelor. Transport Properties of Two-Phase Materials with Random Structure. Annual Review of Fluid Mechanics,6(1974),227-255.
- [4] J. L. Lumley. Two-Phase and Non-Newtonian Flows, In Turbulence. (Edited by P. Bradshaw), Springer-Verlag, Eds.(1978),289-324.
- [5] A. A. Mostafa and H. C. Mongia. On the modelling of turbulent evaporating sprays: Eulerian versus Lagrangian approach. Int. J. Heat and Mass Transfer, 30 (1987).
- [6] M. Hallmann, M. Scheurlen and S. Wittig. Computation of turbulent evaporating sprays: eulerian versus lagrangian approach. Journal of Engineering for Gas Turbines and Power, 117(1)(1995),112-119.

- 
- [7] H. K. Ma, F. H. Lee and M. W. Wang. Numerical study on heat and mass transfer in a liquid-fueled gas turbine combustor. International journal of heat and mass transfer,36(16)(1993).
- [8] W. T. Kim, K. Y. , J. A. Friedman and M. Renksizbulut. Numerical simulation of a steady hollow-cone methanol spray flame within an annular air jet. Combustion Science and Technology, 171(1)(2001),119-139.
- [9] D. Caraeni, C. Bergstrom and L. Fuchs. Modeling of liquid fuel injection, evaporation and mixing in a gas turbine burner using large eddy simulations. Flow, Turbulence and Combustion, 65(2)(2001),223-244.
- [10] B. E. Launder and D. B. Spalding. Mathematical models of turbulence, London academic press, 1972.
- [11] J. C. Beck and A .P. Watkins. The droplet number moments approach to spray modelling: The development of heat and mass transfer sub-models. Int. J. of Heat and Fluid Flow, 24(2003),242-259.
- [12] N. Levy, S. Amara, J.C. Champoussin and N. Guerrasi. Non-Reactive Diesel Spray Computations Supported by PDA Measurements. SAE Technical Paper Series No. 970049.1997



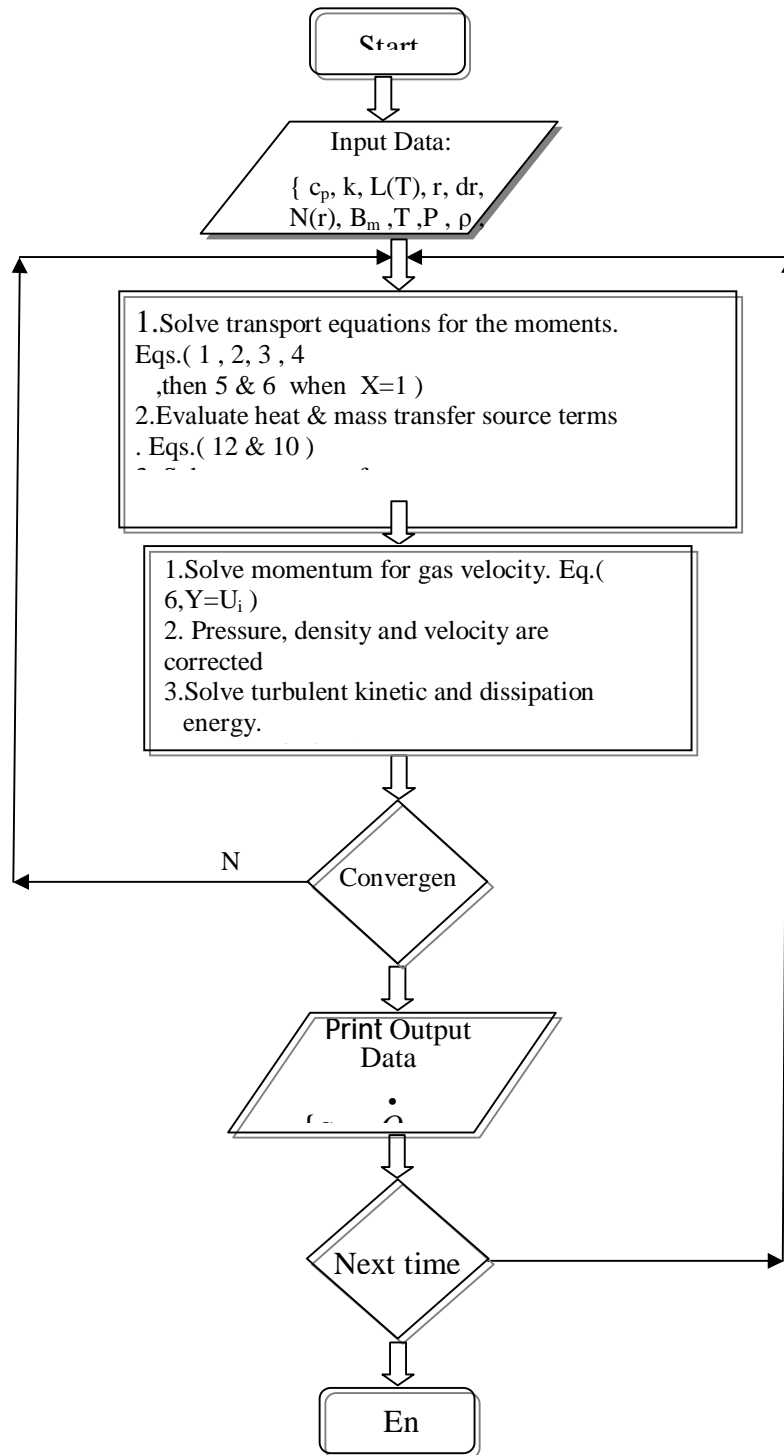


Figure (1): Flow Chart of Fortran program for the solution proceeds at each time step.

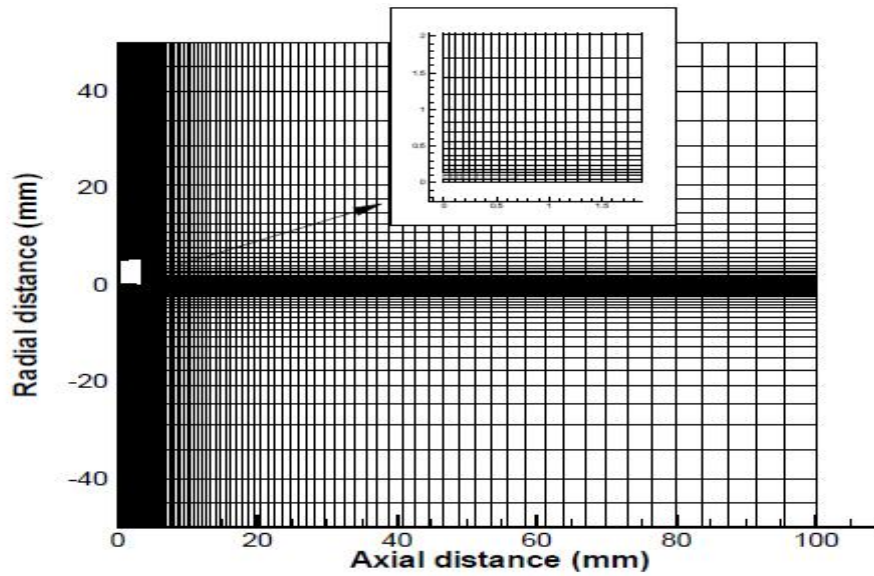


Figure 2: Computational domain.

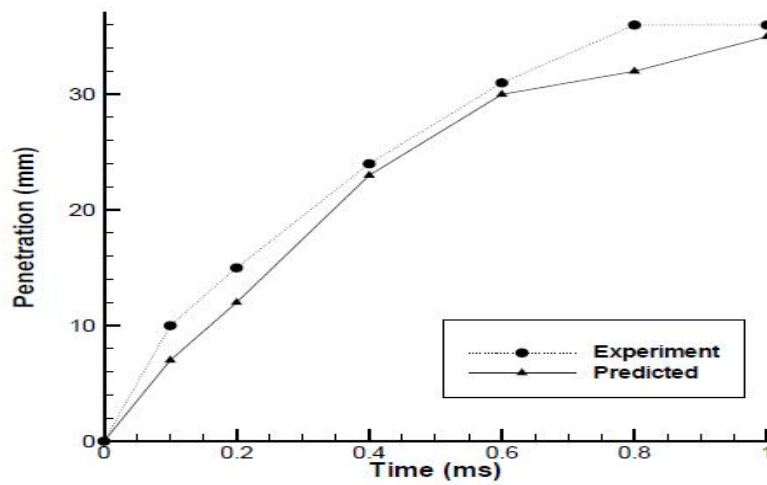


Figure 3: Comparisons of predicted penetration with experimental data.

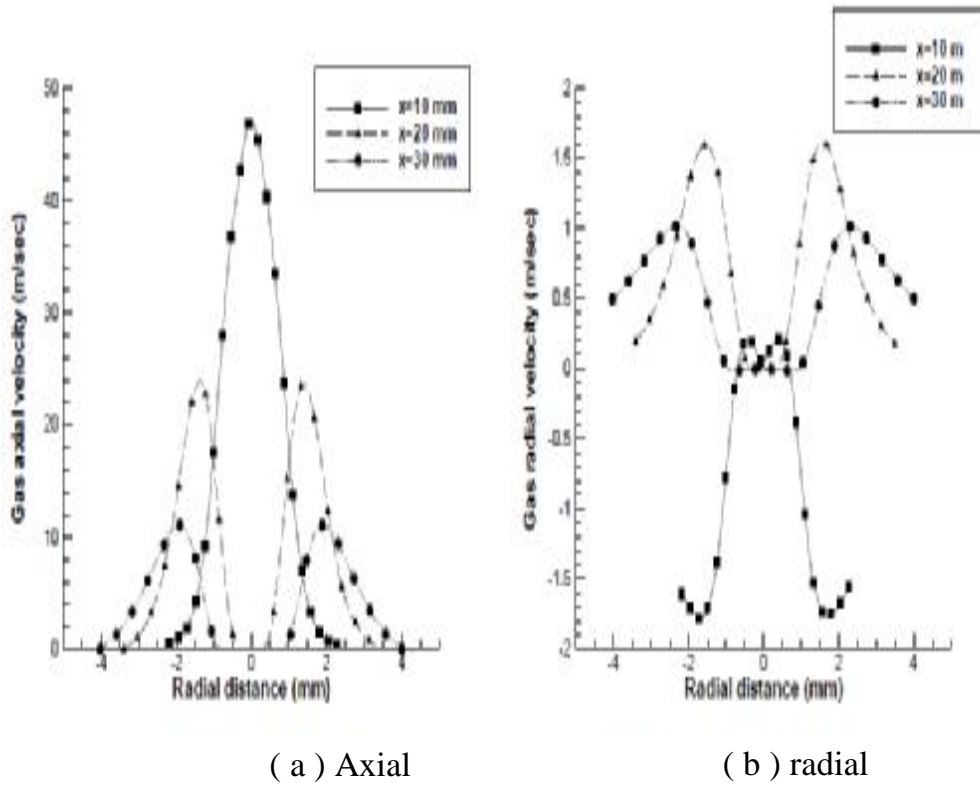


Figure 4: Axial and radial gas velocity at different cross sections at 2 ms.

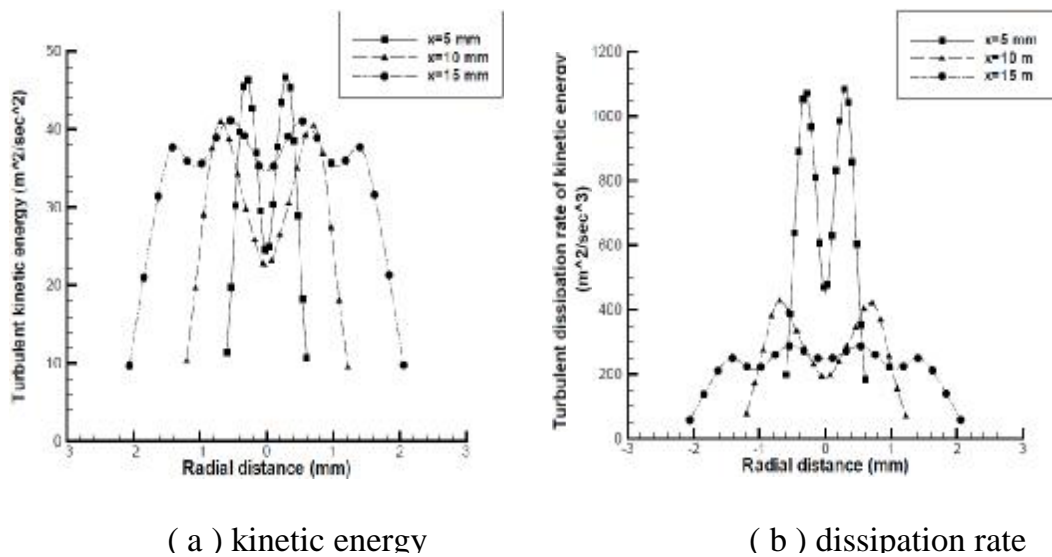


Figure 5: Radial profile of turbulent kinetic and dissipation rate of kinetic energy at different cross-sections at 2ms.